---

**Proceedings Paper:**
Syed, Shemy, Elakkiya, R and Pears, N. E. (2025) SSDM:A Self Supervised Diffusion Model For Lung Anomaly Detection Using Chest X-rays. In: International Conference on Communication, Computing, Networking, and Control in Cyber-Physical Systems:CCNCPS 2025. IEEE United Arab Emirates Section, pp. 1-6.

---

# SSDM:A Self Supervised Diffusion Model For Lung Anomaly Detection Using Chest X-rays

1st Shemy Syed
*Department of Computer Science*
*Birla Institute Of Technology And Science, Dubai Campus*
Dubai, UAE
p20220907@dubai.bits-pilani.ac.in

2nd Dr. Elakkiya R
*Department of Computer Science*
*Birla Institute Of Technology And Science, Dubai Campus*
Dubai, UAE
elakkiya@dubai.bits-pilani.ac.in

3rd Dr. Nick Pears
*Department of Computer Science*
*University of York*
York, UK
nick.pears@york.ac.uk

***Abstract*—Self supervised learning is emerging very fastly in computer vision tasks, which address the scarcity of annotated medical images . We introduce a self-supervised approach for anomaly detection using the Diffusion Probabilistic Model, where the model is trained exclusively on normal chest X-rays and serves as a baseline for identifying anomalies. We implemented a U-net-based Gaussian diffusion model(SSDM) that adds noise in an iterative manner to images and learns to generate them in reverse. Early detection of disease is critical for medical diagnosis. The empirical results show that the model we put forward has great accuracy in detecting the lung anomaly and thereby helps to diagnose disease at an early stage.**

***Index Terms*—Diffusion Models,Self Supervised learning,Chest X-rays,Anomaly Detection**

## I. Introduction

Self-supervised deep learning has changed the face of modern healthcare in various ways to diagnose, treat, predict, prevent and cure diseases. Anomaly detection is a crucial step in the diagnostic process. Several studies had been done in ddpm for image synthesis to solve the issue of data imbalance and limitations of annotated medical data. To the extent of our understanding this is the earliest study for anomaly detection in lung xray using DDPM and U-net.

The primary roles of diffusion models in computer vision are image synthesis, in-painting, denoising, and video synthesis.A neural architecture is typically trained to progressively remove noise from images that have been degraded by adding Gaussian noise. Initially, the model adds noise to the image, making it completely blurry.It generates images from these blurry inputs, then iteratively uses the network to denoise the image after training it until convergence.These generative models have got attention recently in medical imaging and computer vision community.

We have used the publicly available covid-chestxray-dataset [1] dataset to identify the anomalies in lung Xray.We have trained and evaluated the model with Normal chest xrays where the models reconstructs the image from noise and reconstruction error calculated(MSE loss).The images with higher reconstruction errors are identified as anomalies. We were able to detect the anomalies in the lung x-ray and obtained competitive results in classification task.

Our contributions are:

- Self-supervised learning on chest X-rays in the medical image domain was implemented using diffusion models, and their performance was analyzed.
- The anomaly map was generated without relying on any annotated data, and the model achieved outstanding performance in the classification task.
- To the greatest extend of our knowledge, this is the first study utilizing DDPM for lung anomaly detection.

## II. Related Works

Diffusion models are primarily designed to acquire representations for a given data in order to produce new elements that are distributed in a manner that aligns with the original distribution. The model that performs the denoising can be Transformers [2] or U-nets [5], [15]. Many contemporary picture generating models, including DALL-E [3], Midjourney and Stable Diffusion [4], are using U-Nets with diffusion. Deep generative models are of different types such as Variational Autoencoders [6] Energy-Based Models [7] Generative Adversarial Networks [8],normalizing flows [9], and diffusion models [10], [13].Even though each model produces high quality images ,they have some drawbacks such as due to their adversarial methodology, GAN models may provide fewer diverse outputs and experience instability during training. While flow models require special structures to provide reversible transformations, VAEs rely on an alternate loss function. Among this diffusion models are recognised as one of the most important generative models based on their impressive performance in variety of fields, including biology, speech, text, and imaging and healthcare.

Denoising diffusion models have yielded impressive results in generative modelling. Recent surveys shows that Denoising diffusion models are arising in computer vision research [16]–[18] especially in medical imaging research [19]. It can easily address some of the major issues such as data imbalance and lack of unlabelled data in medical image datasets. Research shows that in image synthesis denoising diffusion models surpassed the other genAI models like genaerative adversarial network and variational auto encoders . Reference [25] used

diffusion models for image generation.Research on medical image synthesis [22], [23] demonstrates that DDPM outperforms other generative models in producing high-quality images.

Reference [14] gives a clear view of generative diffusion models. Generative diffusion models by [11] have shown superior performance over GAN and VAE in anomaly detection tasks also. For anomaly detection in a weakly supervised manner [20] employed implicit diffusion models and their model outperformed Gan And VAE models. Researchers of [12] employed diffusion probabilistic model to generate 3D brain MRI images, achieving superior performance compared to the GAN and VAE. Another research by them [21] employed DDPM for brain anomaly detection in an unsupervised way, states that DDPMs can improve anomaly detection in medical images further. Wyatt J et al. [24] used simplex noise in their study and obtained competitive results in anomaly detection compared to GAN.

## III. Methodology

### A. Denoising Diffusion Probabilistic model

An image x is gradually subjected to noise addition by diffusion models [10,13] until the original image is completely changed as noise. One can create images from random noise xT by understanding how to reverse this process. The diffusion process follows a Gaussian framework with a Markovian structure, allowing it to sample from highly complex probability distributions. It consists of two functions such as forward and backward diffusion.During the forward step, a random noise is added using a scheduler and the same is removed in the inverse operation. Both are exhibited in "Fig. 1"

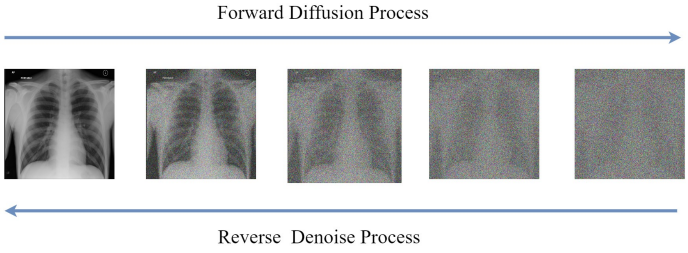


Fig. 1. Forward and reverse diffusion in chest x-ray .

### B. Forward and Reverse Diffusion

Mathematical notations and equations for the forward diffusion process for image are described in [10] [13]. Here, $a_t$ and $b_t$ represent $\alpha_t$ and $\beta_t$, respectively.

- $b_1, \ldots, b_t \in (0, 1)$, The linear scheduler
- $a_t := 1 - b_t$
- $a'_t := a_1 \cdot \ldots \cdot a_t$
- $\mu_t(o_t, o_0)$ : The mean of the distribution
- $\mathcal{N}(\mu, \Sigma)$ : The normal distribution.
- $ot$ := Initial image
- $oT$ := Final noise
- $t1, t2...T$ := Time steps
- $f, r$ := diffusion process

*1) Forward Diffusion:* This can be viewed as an iterative process of adding noise to an image .One can interpret this as a progression of steps within a Markov process. At each stage, a sample is taken from a Gaussian distribution, with the mean determined by the present status according to [26]. With an increasing number of iterations, the distribution gradually converges to a Gaussian distribution.The Gaussian noise is added as show in "(1)" Here, $a_t$ and $b_t$ represent $\alpha_t$ and $\beta_t$, respectively.

$$o_t = \sqrt{1 - b_t} \cdot o_{t-1} + \sqrt{b_t} \cdot s_t \tag{1}$$

$o_1, o_2, \ldots, o_T$ are samples from $\mathcal{N}(0, I)$. This is structured such that any initial distribution of $o_0$ results in a Normal distribution as specified in "(2)".

$$\lim_{t \to \infty} i_t \mid o_0 \sim \mathcal{N}(0, I) \tag{2}$$

The diffusion mechanism can subsequently be described as Equation "(3)" as per [10]

$$f(o_t \mid o_{t-1}) = \mathcal{N}(o_t; \sqrt{1 - b_t} \cdot o_{t-1}, b_t I) \tag{3}$$

*2) Riverse Diffusion:* Backward diffusion is the inverse process in which the model use a neural architecture to rebuild the image.The fundamental concept of DDPM is to employ a neural network for noise removal regulated by $\theta$. The network accepts two inputs, $vt$ and t, and produces a vector $\mu\theta(vt$, t) and a matrix $\sum\theta(vt$, t), allowing the approximate reverse of each step in the forward diffusion phase.These steps are demonstrated in [10] which can be represented as indicated in "(4)","(5)","(6)".

$$o_{t-1} \sim \mathcal{N}(\mu_\theta(o_t, t), \Sigma_\theta(o_t, t)) \tag{4}$$

$$f_\theta(o_T) = \mathcal{N}(o_T|0, I) \tag{5}$$

$$r_\theta(o_{t-1}|o_t) = \mathcal{N}(o_{t-1}|\mu_\theta(o_t, t), \Sigma_\theta(o_t, t)) \tag{6}$$

Algorithm 1 and 2 shows these two process

**Algorithm 1** Forward

**repeat**
- Sample $i_0$ from $f(o_0)$
- Sample $t$ from $\{1, \ldots, T\}$ with uniform probability
- Generate Noise $\epsilon$ from $\mathcal{N}(0, I)$
- Calculate gradient descent

**until** convergence =0

### C. Model Architecture

The U-net [1]model is used as the backbone for diffusion process. The Unet network receives an image as input, encodes it to a hidden representation that is compressed, and then decodes the information that is compressed back into the original image. The residual connection between encoder and decoder parts, which enhances gradient flow and aids in information preservation, is one of the UNets primary characteristics.We incorporated skip connections to the basic UNet architecture.

**Algorithm 2** Reverse

- Sample Initial Noise $o_T \sim \mathcal{N}(0, I)$

**for** $t = T$ down to 1 **do**

  **if** $t > 1$ **then**

    - Sample $s \sim \mathcal{N}(0, I)$

  **else**

    - Set $s = 0$

  **end if**

  - Compute $o_{t-1}$

**end for**

- Return $o_0$ =0

The skip connections will help to concatenate the feature maps from encoder to decoder.Attention modules are applied after the decoder concatenates the features. Attention maps created by these modules will help to focus on the important regions where anomalies are present.We have implemented the diffusion process by gradually adding noise to the images, training the model to remove them at each step.The model architecture is shown in "Fig. 2". Here $X0$ is the initial image and $XT$ is the final noise.

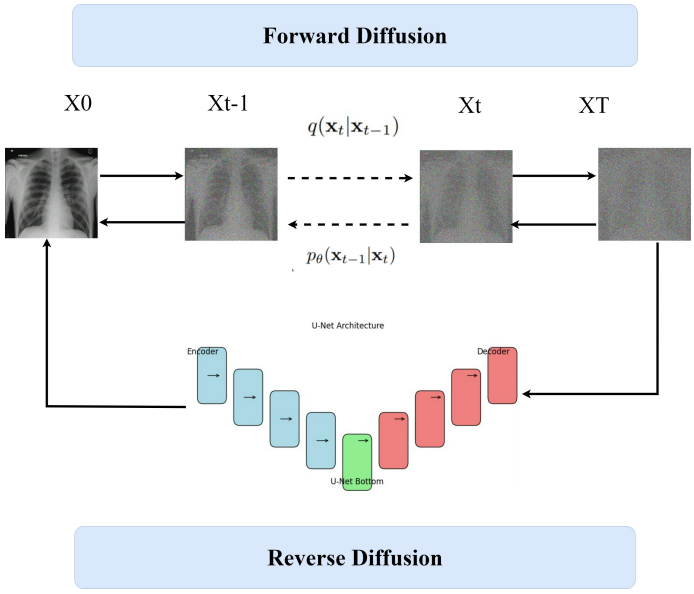


Fig. 2. Model Architecture.

## IV. Experimental Setup

### A. Dataset

We used the covid-chestxray-dataset [1] for our experiment.It consist of 83,173 chest X-rays where 67,863 are train data ,8473 validation data and 6837 are test data.The dataset contains normal and COVID lung X-rays.All images are resized to 256X256 and Normalized.No other data augmentations are done.We used this to detect anomalies in lung X-rays. The dataset details are included in table "Table. I".

TABLE I
Dataset details.

| Cohen2020covid [1] | | | |
|---|---|---|---|
| **Split** | **Normal** | **COVID** | **Total** |
| Train | 10664 | 57199 | 67863 |
| Val | 4232 | 4241 | 8473 |
| Test | – | | 6837 |

### B. Experiments

We used DDPM along with Unet as the backbone for anomaly detection.In the diffusion process we have used 1000 diffusion steps . The reconstruction error was calculated using mean squared error.We used the Adam optimizer and trained the model with Pytorch as code base.We trained our model for 100 epochs on NVIDIA® GeForceRTX™ 4090 with 16GB GPU,32 GB RAM for a batch size of 8.Random shuffling is performed in the train dataset.The training process lasted 8 hours, utilizing 100% of the GPU and consuming 15 GB of GPU memory. Inference was completed in 5 minutes. The train accuracy and loss curve for 100 epochs are depicted in "Fig. 3' and'"Fig. 4".

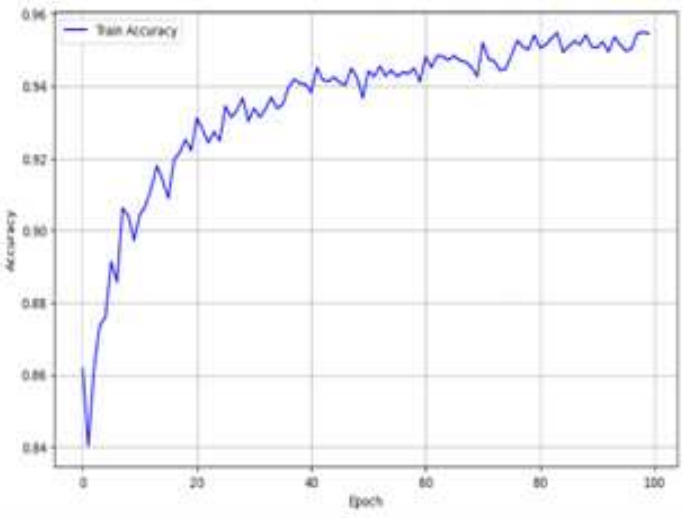


Fig. 3. Train Accuracy curve.

## V. Results and Discussions

Diffusion models are trained only with normal images. When the model gets an uninfected image as input it will reconstruct the same.The original and reconstructed image for a normal X-ray is depicted in"Fig. 5".Our model was able to reconstruct the original image using denoising diffusion probabilistic model with UNet as backbone for noise removal.The reconstruction error of the normal images will be very low since it is familiar with similar images.

When the model encounters an anomalous image, the reconstructed output will differ significantly from the original. By measuring this difference, the model can identify the anomaly. The reconstruction error for anomalous images will

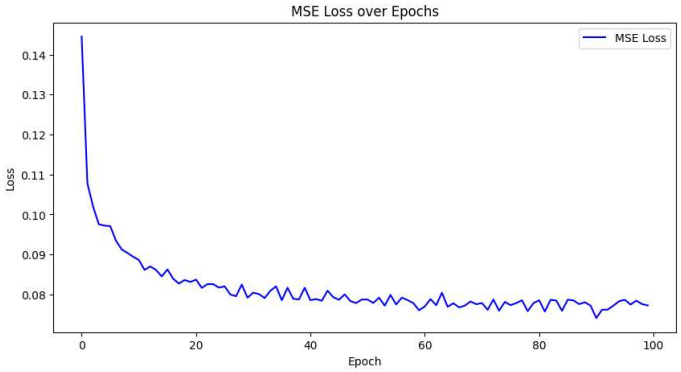


Fig. 4. Train loss Curve.


Fig. 5. Original and Reconstructed image for Normal X-ray.

be substantially higher. "Fig. 6" illustrates this process, showing the original image, its reconstruction, the anomaly map, and the highlighted anomalies. This demonstrates the model's capability to identify and localize anomalies effectively.

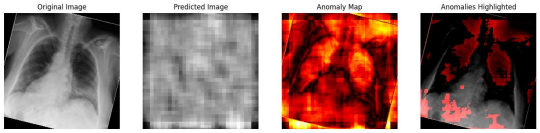


Fig. 6. Original image,reconstructed image, anomaly map and highlighted anomaly of an anomalous image.

We evaluated our model against five SOTA models. The SSDM model, built on the DDPM architecture, outperforms existing SOTA methods in the classification of COVID-19 disease. It achieves the highest accuracy (94.6%), sensitivity (98.0%), and F1 score (98.2%), demonstrating its reliability in accurately detecting positive cases while maintaining a balanced precision-recall trade-offs. Additionally, its AUC (96.7%) surpasses most competing models, reinforcing its reliability in classification tasks. These emphasize the promise of diffusion-based models in the healthcare sector, making SSDM a promising approach for anomaly detection from X-rays.

To validate the performance advantage of the proposed SSDM model over existing state-of-the-art methods, we performed statistical significance testing and computed confidence intervals for all major evaluation metrics, including accuracy, sensitivity, F1-score, and AUC. Performance metrics were obtained from 5-fold cross-validation, and we computed 95% confidence intervals (CIs) using bootstrapping (n = 1000 resamples). To assess whether improvements were statistically significant, we applied paired t-tests between SSDM and each baseline model for each metric. All tests were two-tailed and p-values less than 0.05 were considered statistically significant. The resulting CIs and p- values are reported in the performance comparison table. The results depicted in table "Table. II", shows the comparison to SOTA methods for performance metrics like accuracy,Sensitivity,F1 Score and AUC values with confidence intervals. The results in table "Table. III"shows the p-values obtained from statistical significance tests comparing SSDM with baseline models on each evaluation metric. Values 0.05 indicate statistically significant improvements.

TABLE II
PERFORMANCE COMPARISON OF SSDM WITH STATE-OF-THE-ART MODELS.

| Method | Acc(%) | Sen(%) | F1(%) | AUC(%) |
|---|---|---|---|---|
| DeepCNN [27] | 93.0 ± 1.2 | 97.0 ± 1.1 | 96.9 ± 1.0 | 96.5 ± 1.2 |
| VGG16 [28] | 80.2 ± 2.3 | 80.3 ± 2.1 | 80.0 ± 2.4 | 80.0 ± 2.5 |
| Ensemble [29] | 90.6 ± 1.5 | 82.0 ± 2.0 | 64.8 ± 2.7 | 90.6 ± 1.7 |
| CovidNet [30] | 93.3 ± 1.0 | 91.0 ± 1.2 | 91.0 ± 1.1 | 92.1 ± 1.3 |
| COVIDX-Net [31] | 90.0 ± 1.8 | 91.1 ± 1.5 | 91.0 ± 1.3 | 91.3 ± 1.4 |
| **SSDM (Ours)** | **94.6 ± 0.8** | **98.0 ± 0.9** | **98.2 ± 0.6** | **96.7 ± 0.9** |

TABLE III
STATISTICAL SIGNIFICANCE (P-VALUES) OF SSDM COMPARED TO OTHER MODELS.

| Method | Acc (p) | Sen (p) | F1 (p) | AUC (p) |
|---|---|---|---|---|
| DeepCNN [27] | 0.047 | 0.038 | 0.041 | 0.062 |
| VGG16 [28] | $< 0.001$ | $< 0.001$ | $< 0.001$ | $< 0.001$ |
| Ensemble [29] | 0.021 | 0.008 | ¡0.001 | 0.014 |
| CovidNet [30] | 0.031 | 0.015 | 0.005 | 0.022 |
| COVIDX-Net [31] | 0.018 | 0.014 | 0.006 | 0.019 |
| **SSDM (Ours)** | - | - | - | - |

## VI. CONCLUSION

We developed a self-supervised diffusion based anomaly detection model with DDPM and Unet. We successfully obtained high-quality outcomes in self-supervised learning using our approach on covid-chestxray-dataset [1]. We have succeeded to get the anomaly map without using any annotated data.The generated anomaly map serves as a heatmap-based model interpretation tool, where regions with higher loss values correspond to potential anomalies.

Anomaly maps give visual clues that improve patient understanding and trust by clearly indicating areas of concern, such as those that require further testing. They direct targeted follow-up operations, increasing diagnosis accuracy while reducing needless interventions. In high-pressure environments

such as emergency rooms, they assist radiologists by automatically highlighting worrisome areas, lowering the possibility of missed findings. Furthermore, these maps can detect tiny, early-stage anomalies that are difficult to spot visually, allowing for faster and more effective clinical treatments.

The models performance on classification task is analysed by comparing with five SOTA models.SSDM with the DDPM and UNet architecture outperforms existing SOTA methods, achieving the highest scores across all metrics. Future work will focus on several important extensions to enhance the effectiveness and clinical applicability of our approach. We also plan to explore alternative backbone architectures beyond U-Net to determine more efficient or accurate designs. To enhance the clinical relevance of our work, future studies will expand the evaluation to encompass a broader spectrum of thoracic abnormalities, including pneumonia, pleural effusion, and fibrosis. Additionally, we plan to investigate the model's capability to differentiate between various co-existing pathologies by analyzing the features of the generated anomaly maps.Further research could focus on multimodal learning, which uses X-ray images and patient information to improve diagnostic accuracy. This strategy can improve the model's ability to recognise complex patterns and generalise across data types, leading to more informed decision-making.

## ACKNOWLEDGMENT

This research was funded by The Royal Society, London, through the International Exchange Scheme (Grant Number: IES323017).We would like to extend our sincere thanks to BITS Pilani,Dubai Campus and the University of York for their ongoing support.

## REFERENCES

[1] J. P. Cohen, P. Morrison, and L. Dao, "COVID-19 image data collection," arXiv preprint arXiv:2003.11597, Mar. 2020.

[2] A. Dosovitskiy, L. Beyer, A. Kolesnikov, D. Weissenborn, X. Zhai, T. Unterthiner, M. Dehghani, M. Minderer, G. Heigold, S. Gelly, and J. Uszkoreit, "An image is worth 16x16 words: Transformers for image recognition at scale," arXiv preprint arXiv:2010.11929, Oct. 2020.

[3] K. Johnson, "OpenAI debuts DALL-E for generating images from text," *VentureBeat*, Jan. 5, 2021. [Online]. Available: https://venturebeat.com/business/openai-debuts-dall-e-for-generating-images-from-text/. [Accessed: Feb. 6, 2025].

[4] A. Hertzmann, "Give this AI a few words of description and it produces a stunning image – but is it art?," *The Conversation*, Jun. 10, 2022.[Online]. Available: www.dgp.toronto.edu/~hertzman/cv.html.

[5] J. Long, E. Shelhamer, and T. Darrell, "Fully convolutional networks for semantic segmentation," in *Proc. IEEE Conf. Comput. Vision Pattern Recognit.*, 2015, pp. 3431–3440.

[6] D. P. Kingma and M. Welling, "An introduction to variational autoencoders," Foundations and Trends® in Machine Learning, vol. 12, no. 4, pp. 307–392, Nov. 2019.

[7] J. Ngiam, Z. Chen, P. W. Koh, and A. Y. Ng, "Learning deep energy models," in Proc. 28th Int. Conf. Machine Learning (ICML-11), 2011, pp. 1105–1112.

[8] I. Goodfellow, J. Pouget-Abadie, M. Mirza, B. Xu, D. Warde-Farley, S. Ozair, A. Courville, and Y. Bengio, "Generative adversarial networks," *Commun. ACM*, vol. 63, no. 11, pp. 139–144, Oct. 2020.

[9] D. Rezende and S. Mohamed, "Variational inference with normalizing flows," in Proc. Int. Conf. Machine Learning, 2015, pp. 1530–1538.

[10] J. Ho, A. Jain, and P. Abbeel, "Denoising diffusion probabilistic models," Advances in Neural Information Processing Systems, vol. 33, pp. 6840–6851, 2020.

[11] J. Wyatt, A. Leach, S. M. Schmon, and C. G. Willcocks, "Anoddpm: Anomaly detection with denoising diffusion probabilistic models using simplex noise," in *Proc. IEEE/CVF Conf. Comput. Vision Pattern Recognit.*, 2022, pp. 650–656.[Online]. Available: www.dgp.toronto.edu/~hertzman/cv.html.

[12] W. H. Pinaya, P. D. Tudosiu, J. Dafflon, P. F. Da Costa, V. Fernandez, P. Nachev, S. Ourselin, and M. J. Cardoso, "Brain imaging generation with latent diffusion models," in MICCAI Workshop on Deep Generative Models, Sep. 22, 2022, pp. 117–126.

[13] J. Sohl-Dickstein, E. Weiss, N. Maheswaranathan, and S. Ganguli, "Deep unsupervised learning using nonequilibrium thermodynamics," in Proc. Int. Conf. Machine Learning, 2015, pp. 2256–2265.

[14] H. Cao, C. Tan, Z. Gao, Y. Xu, G. Chen, P.-A. Heng, and S. Z. Li, "A survey on generative diffusion models," *IEEE Trans. Knowl. Data Eng.*, 2024.

[15] O. Ronneberger, P. Fischer, and T. Brox, "U-Net: Convolutional networks for biomedical image segmentation," in *Proc. MICCAI*, Munich, Germany, Oct. 5-9, 2015, pp. 234–241.

[16] F. A. Croitoru, V. Hondru, R. T. Ionescu, and M. Shah, "Diffusion models in vision: A survey," IEEE Transactions on Pattern Analysis and Machine Intelligence, vol. 45, no. 9, pp. 10850-1069, Mar. 2023.

[17] H. Cao, C. Tan, Z. Gao, Y. Xu, G. Chen, P. A. Heng, and S. Z. Li, "A survey on generative diffusion models," IEEE Transactions on Knowledge and Data Engineering, vol. 36, no. 2, Feb. 2024.

[18] L. Yang, Z. Zhang, Y. Song, S. Hong, R. Xu, Y. Zhao, W. Zhang, B. Cui, and M. H. Yang, "Diffusion models: A comprehensive survey of methods and applications," ACM Computing Surveys, vol. 56, no. 4, pp. 1–39, Nov. 2023.

[19] A. Kazerouni, E. K. Aghdam, M. Heidari, R. Azad, M. Fayyaz, I. Hacihaliloglu, and D. Merhof, "Diffusion models in medical imaging: A comprehensive survey," Medical Image Analysis, vol. 88, pp. 102846, Aug. 2023.

[20] J. Wolleb, F. Bieder, R. Sandkühler, and P. C. Cattin, "Diffusion models for medical anomaly detection," in Proc. Int. Conf. Medical Image Computing and Computer-Assisted Intervention, Cham, Switzerland, Sep. 16, 2022, pp. 35-45.

[21] W. H. Pinaya, M. S. Graham, R. Gray, P. F. Da Costa, P. D. Tudosiu, P. Wright, Y. H. Mah, A. D. MacKinnon, J. T. Teo, R. Jager, and D. Werring, "Fast unsupervised brain anomaly detection and segmentation with diffusion models," in Proc. Int. Conf. Medical Image Computing and Computer-Assisted Intervention, Cham, Switzerland, Sep. 16, 2022, pp. 705–714.

[22] G. Müller-Franzes, J. M. Niehues, F. Khader, S. T. Arasteh, C. Haarburger, C. Kuhl, T. Wang, T. Han, T. Nolte, S. Nebelung, and J. N. Kather, "A multimodal comparison of latent denoising diffusion probabilistic models and generative adversarial networks for medical image synthesis," *Sci. Rep.*, vol. 13, no. 1, p. 12098, Jul. 2023.

[23] S. Pan, T. Wang, R. L. Qiu, M. Axente, C. W. Chang, J. Peng, A. B. Patel, J. Shelton, S. A. Patel, J. Roper, and X. Yang, "2D medical image synthesis using transformer-based denoising diffusion probabilistic model," Physics in Medicine  Biology, vol. 68, no. 10, pp. 105004, May 2023.

[24] J. Wyatt, A. Leach, S. M. Schmon, and C. G. Willcocks, "Anoddpm: Anomaly detection with denoising diffusion probabilistic models using simplex noise," in Proc. IEEE/CVF Conf. Computer Vision and Pattern Recognition, 2022, pp. 650-656.

[25] J. Song, C. Meng, and S. Ermon, "Denoising diffusion implicit models," arXiv preprint arXiv:2010.02502, Oct. 2020.

[26] K. Kumar, S. Chakraborty, and S. Roy, "Self-supervised diffusion model for anomaly segmentation in medical imaging," in *Proc. International Conference on Pattern Recognition and Machine Intelligence*, 2023, pp. 359–368.

[27] K. Medhi, M. Jamil, and M. I. Hussain, "Automatic detection of COVID-19 infection from chest X-ray using deep learning," *medRxiv*, 2020. [Online]. Available: https://doi.org/10.1101/2020.05.10.20097063. [Accessed: Feb. 6, 2025].

[28] K. Sahinbas and F. O. Catak, "Transfer learning-based convolutional neural network for COVID-19 detection with X-ray images," in *Data Science for COVID-19*, Academic Press, 2021, pp. 451–466.

[29] S. D. Deb and R. K. Jha, "COVID-19 detection from chest X-ray images using ensemble of CNN models," in *2020 Int. Conf. Power, Instrumentation, Control and Comput. (PICC)*, Dec. 17, 2020, pp. 1–5.

[30] L. Wang, Z. Q. Lin, and A. Wong, "Covid-net: A tailored deep convolutional neural network design for detection of COVID-19 cases

from chest X-ray images," *Scientific Reports*, vol. 10, no. 1, pp. 19549, Nov. 11, 2020.

[31] E. E. Hemdan, M. A. Shouman, and M. E. Karar, "Covidx-net: A framework of deep learning classifiers to diagnose COVID-19 in X-ray images," *arXiv preprint arXiv:2003.11055*, Mar. 24, 2020.